Available online at www.sciencedirect.com
SCIENCE DIRECT®
Materials Science and Engineering C 23 (2003) 903–908
MATERIALS SCIENCE & ENGINEERING C
www.elsevier.com/locate/msec

Interfacially organized DNA/polycation complexes: a route to new planar polymeric and composite nanostructures

G.B. Khomutov[a,*], M.N. Antipina[a], R.V. Gainutdinov[b], V.V. Kislov[c], A.A. Rakhnyanskaya[d], A.N. Sergeev-Cherenkov[a], A.L. Tolstikhina[b], T.V. Yurova[a]

[a] *Faculty of Physics, Moscow State University, 119992 Moscow, Russia*
[b] *Institute of Crystallography RAS, 119899 Moscow, Russia*
[c] *Institute of Radioengineering and Electronics RAS, 101999 Moscow, Russia*
[d] *Department of Chemistry, Moscow State University, 119992 Moscow, Russia*

Abstract

Effects of nano-scale supramolecular organization and patterning in amphiphilic polycation monolayer formed by poly-4-vinilpyridine with 16% cetylpyridinium groups and in novel planar DNA/amphiphilic polycation complexes formed at the air-aqueous DNA solution interface and deposited on the solid substrates have been studied using AFM. Stable ordered quasi-crystalline planar polymeric monolayer structures were formed by amphiphilic polycation molecules. Extended net-like and quasi-circular toroidal condensed conformations of deposited planar DNA/amphiphilic polycation complexes were obtained in dependence on the amphiphilic polycation Langmuir monolayer state during the DNA binding. Those monolayer and multilayer DNA/polycation complex Langmuir–Blodgett films were used as templates and nanoreactors for generation of inorganic nanostructures. As a result, ultrathin polymeric nanocomposite films with integrated DNA building blocks and inorganic semiconductor (CdS) and iron oxide nanoparticle quasi-linear arrays or aggregates (nanorods) were formed successfully and characterized by TEM. The data obtained give evidence for effectiveness of the monolayer techniques for study mechanisms of DNA structural transformations caused by complexation with cationic compounds and demonstrate its perspectives for creation of new planar DNA-based self-organized stable polymeric complex nanostructures and nanocomposites with nano-scale structural ordering.

Keywords: Nucleic acids; Polycation; Complex; Liquid–gas interface; Monolayer; Nanoparticles; CdS; Iron oxide; Nanostructures

1. Introduction

A wide range of natural biological structures including nucleic acids demonstrate remarkable properties for self-assembly, self-organization and self-replication. Learning the mechanisms of biomolecular organization and assembly processes, and application of these principles to design and fabrication of new functional molecular nanostructures and nanostructured materials can be an effective approach in nanoscale science, advanced materials research and nanotechnology. Polymeric and composite materials are widely used currently in conventional technologies and industry. Cost-effective synthesis and assembling of polymeric and nanocomposite materials and films with controlled composition and structural organization down to the nano-scale level of individual molecules is a challenge now with potential for new generation of advanced functional materials and coatings. Fabrication and study of organized hybrid nanostructures with integrated biological, polymeric and/or inorganic building blocks can be important for nano-biotechnological applications. It can result in development of materials with high functional specificity and effectiveness characteristic for biological systems along with enhanced processability and applicability due to the synthetic polymeric and inorganic components. DNA molecules are promising candidates for nanobiotechnology building blocks to construct nano-scale wires, scaffolds and frameworks due to the unique DNA recognition capabilities, physicochemical and mechanical stability, and synthetic availability of practically any desired nucleotide sequences and lengths [1]. Based on hybridization of DNA oligomers, gold nanoparticles were assembled to supramolecular aggregates [2]. Metallic nanowires, metallic and semiconductor nanoparticles were fabricated and arranged via DNA tem-

* Corresponding author. Tel.: +7-95-939-3007; fax: +7-95-939-1195.
E-mail address: gbk@phys.msu.ru (G.B. Khomutov).

0928-4931/$ - see front matter © 2003 Elsevier B.V. All rights reserved.
doi:10.1016/j.msec.2003.09.090

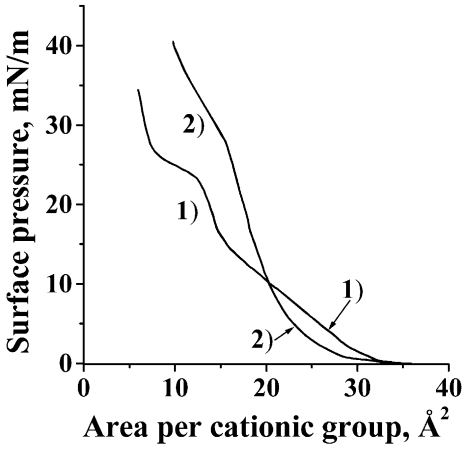

Fig. 1. Surface pressure-monolayer area isotherms of Langmuir monolayer formed by amphiphilic polycation PVP-16 on the pure water subphase (pH = 6) (Curve 1), and on the aqueous DNA solution (DNA concentration 1.2×10^{-4} M (for monomer), 1 mM NaCl, pH = 6) (Curve 2).

plating [3–13]. Starting from pioneering work [14], atomic force microscopy (AFM) was widely used for investigation of immobilized DNA molecules and complexes.

In this work, we present our results on the development of new synthetic nanomanufacturing methods based on the interfacial monolayer nanofabrication strategies. Novel ultrathin planar polymeric nanoscale-ordered quasi-crystalline films and controlled-morphology planar polymeric complexes with DNA were formed. Those monolayer and multilayer DNA/amphiphilic polycation complex Langmuir–Blodgett (LB) films were used as templates and nanoreactors for generation of inorganic nanostructures (semiconducting CdS and iron oxide nanoparticle quasi-linear arrays or aggregates). The obtained nanostructures were characterized by AFM and transmission electron microscopy (TEM) techniques.

2. Experimental

Stearic acid (SA), arachidic acid (AA), $CdCl_2$, $FeCl_3$ and salmon thimus native DNA (Na salt) were obtained from Sigma and used as supplied. Amphiphilic polycation poly-4-vinilpyridine (PVP) with 16% cetylpiridinium groups (PVP-16) was synthesized via the known procedures [15]. PVP with polymerization degree 1100 was prepared and then quaternized with cetyl bromide. Polymer composition was determined by IR spectroscopy measurements. Positive charges in PVP-16 molecules in contact with aqueous phase at neutral pH values are due to the quaternary ammonium groups, what in combination with hydrophobic groups makes that polymer molecule water-insoluble and amphiphilic. Milli-Q water purification system was used to produce water

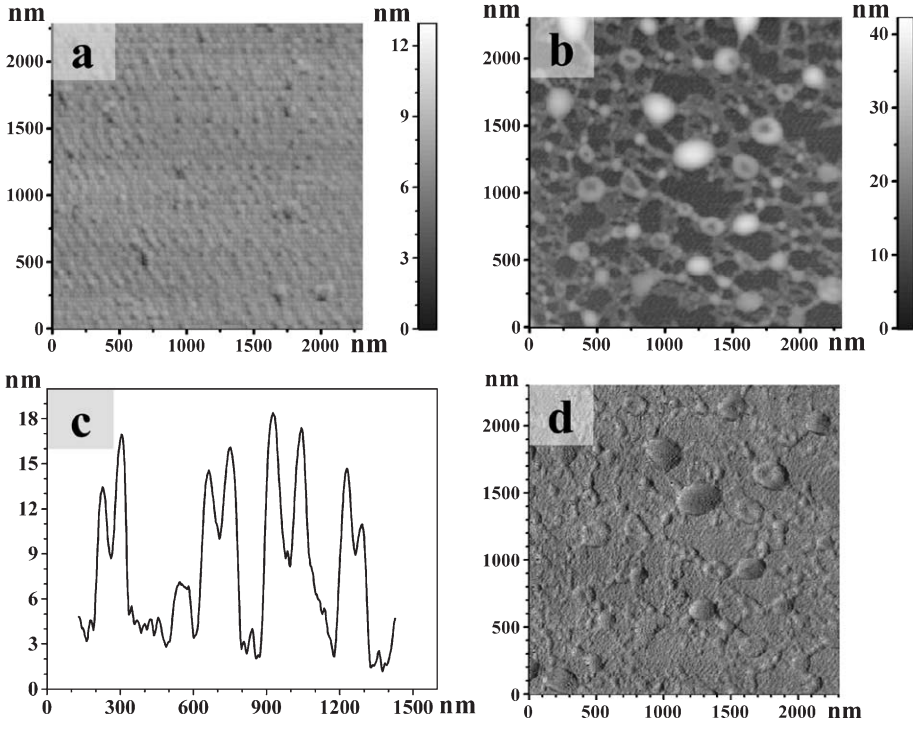

Fig. 2. AFM tapping mode images of two-layer LB films deposited onto the mica substrate. Image (a): top view topographic image of PVP-16 LB film deposited after 10 min incubation of the PVP-16 Langmuir monolayer at low surface pressure value ($\pi \cong 0$) on the water subphase surface (pH = 6) (image size 2300 nm × 2300 nm). Image (b): top view topographic images of DNA/PVP-16 complex LB film. Complex formation conditions: PVP-16 monolayer surface pressure value 20 mN/m during the DNA binding, incubation time 25 min on the surface of aqueous subphase with composition: 1.2×10^{-4} M DNA (for monomer), 1 mM NaCl, pH = 6 (image size, 2300 × 2300 nm). Curve (c): characteristic cross-section profile of the image (b) parallel to the *X*-axis. Image (d): AFM phase contrast mode top view image corresponding to the image (b).

with an average resistivity of 18 MΩ cm for all experiments. Surface pressure–monolayer area (π–A) isotherm measurements and monolayer deposition onto the solid substrates were carried out on a fully automatic conventional Teflon trough at 21 °C as described elsewhere [16]. Langmuir monolayers were formed by spreading a chloroform solution of surfactant on the surface of the aqueous phase (pH = 6). Monolayers were transferred from the surface of aqueous subphase to the solid substrates at a constant surface pressure ($\pi \sim 20$ mN/m), temperature (21 °C) and dipping speed (5 mm/min) using conventional vertical substrate dipping method to form mono- and multilayer LB films. Mica substrates were used for AFM investigations and were freshly cleaved immediately before monolayer deposition. Samples for TEM measurements were prepared by monolayer deposition from aqueous subphase surface onto the Formwar film supported by the copper grid.

Iron oxide nanoparticles were generated via the incubation of corresponding precursor film containing Fe^{3+} cations (Fe^{3+}-arachidate LB film and DNA/Fe^{3+}/PVP-16 complex film) in the sodium borohydride (5×10^{-4} M) or ascorbic acid (1×10^{-3} M) solutions followed by the film incubation in the high pH aqueous media (pH = 10) at ambient conditions for 1 or 2 h. The preliminary analyses of the generated iron-containing nanoparticles using electron diffraction technique pointed to the iron oxide nature (magnetite and maggemite phases) of obtained nanoparticles. Fe^{3+}-containing five-layer AA LB films were formed by the vertical lifting deposition of arachidic acid monolayer from the $FeCl_3$ solution (2×10^{-4} M $FeCl_3$, pH = 2.5) onto the substrate surface. DNA/Fe^{3+}/PVP-16 complex film was formed via the incubation of DNA/PVP-16 complex LB film in the $FeCl_3$ solution (2×10^{-4} M $FeCl_3$, pH = 2.5).

Semiconductor CdS nanoparticles were synthesized via the incubation of corresponding precursor film containing Cd^{2+} cations (cadmium stearate LB film and DNA/Cd^{2+}/PVP-16 complex film) in the H_2S atmosphere for 2 h. DNA/Cd^{2+}/PVP-16 complex film was formed via the incubation of DNA/PVP-16 LB film in the $CdCl_2$ solution (2×10^{-4} M $CdCl_2$, pH = 6.0) for 1 h. Cadmium stearate five-layer LB films were formed by the vertical lifting deposition of SA monolayer from the $CdCl_2$ solution (4×10^{-4} M $CdCl_2$, pH = 6.0) onto the substrate surface.

AFM measurements were performed with the use of Solver P47-SPM-MDT scanning probe microscope (NT MDT, Moscow, Russia) in a tapping mode. Silicon cantilevers NSC11 (Estonia, Mikromasch) with the tip-radii of about 10 nm were used. Images were measured in air at ambient temperature (21 °C) and were stable and reproducible.

TEM images were obtained with the use of Jeol JEM-100B microscope.

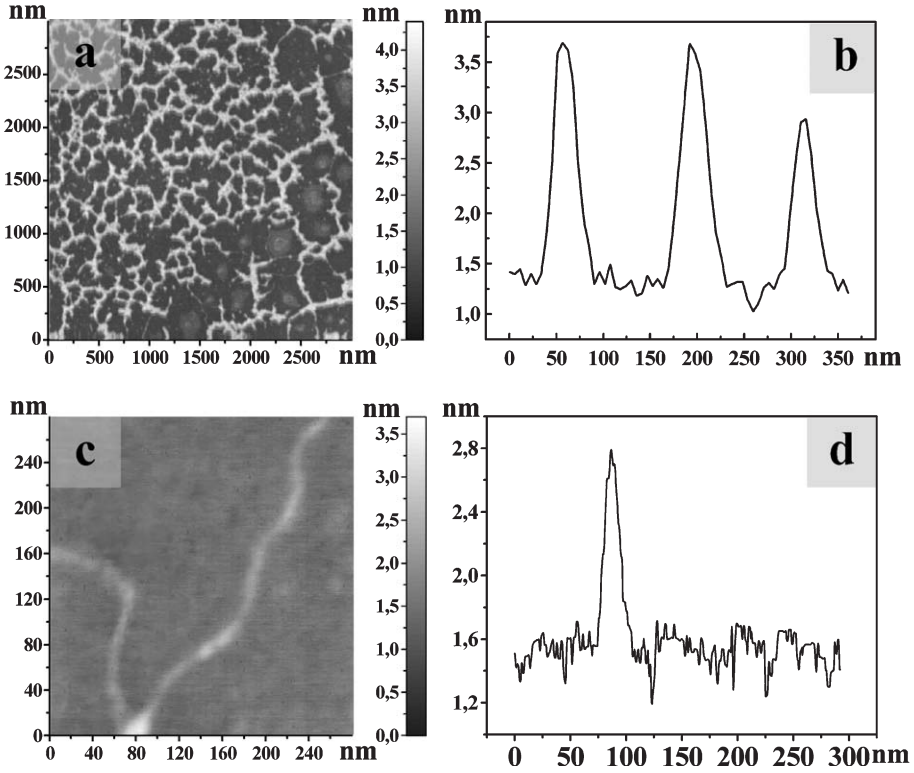

Fig. 3. AFM tapping mode top view topographic images of DNA/PVP-16 complex two-layer LB film on the mica substrate. Complex formation conditions: PVP-16 monolayer surface pressure value ~ 0 during the DNA binding, incubation time 25 min. The composition of the aqueous subphase was 1.2×10^{-4} M DNA (for monomer), 1 mM NaCl, pH = 6. Image (a): image size 3000 × 3000 nm. Curve (b): characteristic cross-section profile of the image (a). Image (c): single DNA molecule bound with PVP-16 monolayer, image size: 280 × 280 nm. Curve (d): characteristic cross-section profile of the image (c).

3. Results and discussion

Characteristic compression isotherms of Langmuir monolayer formed by amphiphilic polycation PVP-16 on the pure water subphase and on the aqueous DNA solution are shown on Fig. 1 (curves 1 and 2, correspondingly). Interaction of negatively charged DNA molecules with cationic amphiphile polymer molecules and interfacial DNA/PVP-16 complex formation resulted in characteristic changes of the monolayer π–A isotherm—decrease of surface pressure values in high monolayer area region and increase in the slope of the isotherm at lower area values (Curve 2).

Fig. 2a demonstrates typical AFM tapping mode top view image of two-layer PVP-16 LB film deposited after 10 min incubation of the PVP-16 Langmuir monolayer at low surface pressure value ($\pi \cong 0$). One can see the ordered fine structure of the amphiphilic polyelectrolyte film with quasi-linear organization of structural elements ($\sim$ 30 nm wide, 2 nm height) in the film. That structure can be a result of the organized surface micelle arrays formation which is known for LB films of diblock copolymers [17]. The characteristic ordered organization of surface micelles in PVP-16 LB film can be a result of smectic liquid crystal ordering of linear PVP-16 molecules on the aqueous surface due to the effective electrostatic repulsive interaction between the positively charged links and extended polycation molecules.

Fig. 2b,c shows the structure of DNA/PVP-16 complexes formed in the case when compressed PVP-16 monolayer with quasi-homogeneous positively charged surface interacted with DNA molecules from the aqueous phase. Planar quasi-circular toroidal structures bound by fibers are clearly seen on the Fig. 2b,d. Such toroidal morphologies are known for compacted DNA structures [18]. The diameter of toroids can be evaluated from the characteristic cross-section profile of the image b (curve c on Fig. 2) and is about 200 nm.

Substantially different morphology of the DNA/PVP-16 complex film—planar net-like or lattice structure—was obtained when DNA molecules interacted with uncompressed PVP-16 monolayer (Fig. 3a). In that case DNA molecules from the aqueous bulk subphase interact with individual PVP-16 molecules which are separated maximally from each other in the monolayer due to the electrostatic repulsive interactions. The effective surface concentration of PVP-16 molecules interacting with DNA molecules (which are at the constant concentration in the bulk aqueous phase) can be easily changed and adjusted controllably by variation of the PVP-16 Langmuir monolayer area. The anionic phosphate groups in a double-stranded DNA are charged to a degree of about one negative charge every 3.5 Å at low ionic strength [19,20]. That linear charge density is substantially higher than the linear charge density value of one positive charge per $\sim$ 2.5 nm in the extended PVP-16 molecule. As a result, individual PVP-16 molecule can not neutralize bound DNA molecule and the overcharging effects and multimolecular cross-binding of linear stretched DNA and PVP-16 molecules can occur at the air-aqueous phase interface with formation of structures organized as interconnected DNA/PVP-16 complexes with extended conformation in which DNA and PVP-16 molecules form a bundle net-like planar superstructures. The height value of the complex derived from cross-section profile (Fig. 3b) is close to that measured by AFM in DNA multistranded aggregated structures ($\sim$ 2.1 nm) [21]. Characteristic fine structure of ordered close-packed surface micelles visible in Fig. 2a,b is absent in Fig. 3 giving evidence for practically complete incorporation of PVP-16 molecules in planar net-like multimolecular complexes with DNA. Single stretched DNA molecules bound with PVP-16 monolayer were also observed (Fig. 3c). Characteristic cross-section profile of the image 3c gives the height value of the extended object of about 1 nm what corresponds to the height of double-stranded DNA molecule on a solid substrate measured by AFM in air (typically 0.5–1 nm) [22–24].

Fig. 4 demonstrates TEM micrographs showing iron oxide nanoparticles synthesized in multilayer ferrous arachidate LB film. One can see the formation of disordered arrays of large nanoparticles (Fig. 4a) and massive aggre-

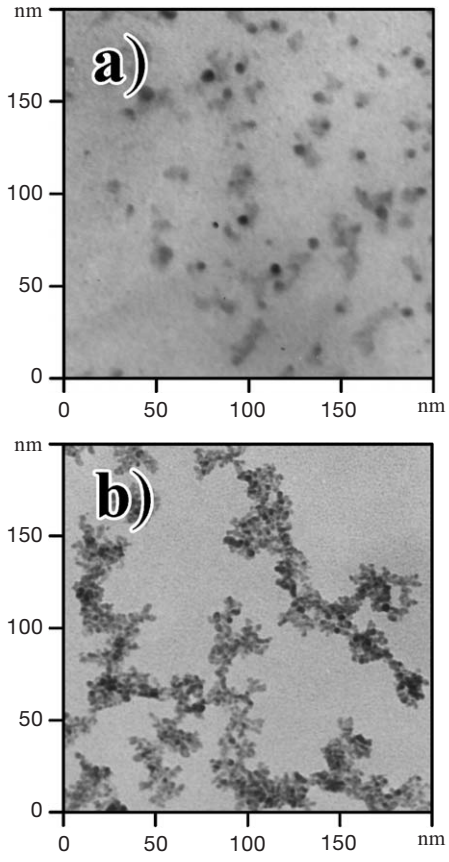

Fig. 4. Transmission electron micrographs showing iron oxide nanoparticles synthesized in multilayer ferrous arachidate LB film. Image (a): $NaBH_4$ (5×10^{-4} M) was used as a reductant. Image (b): ascorbic acid (10^{-3} M) was used as a reductant.

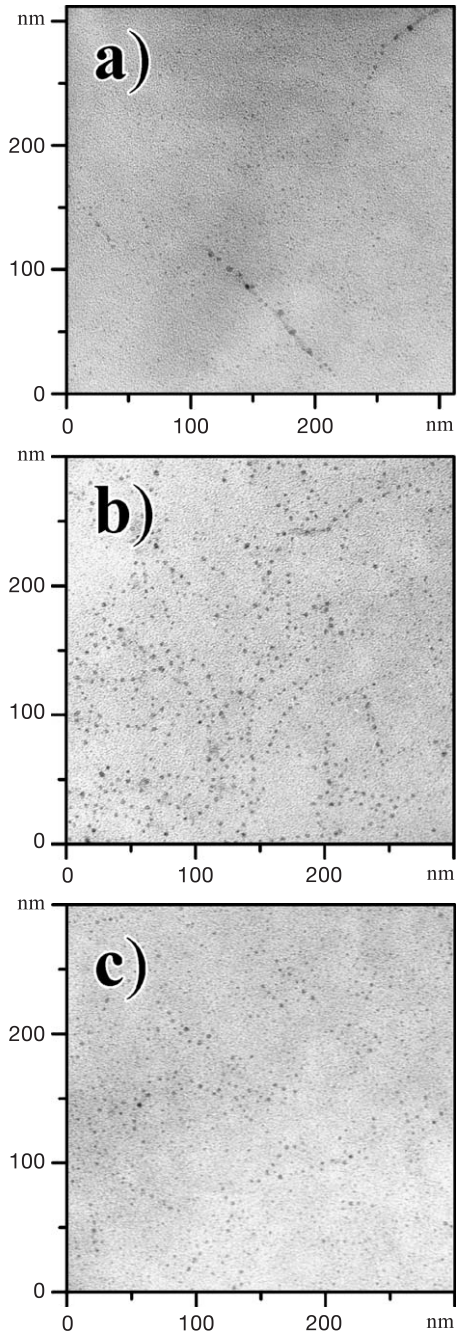

Fig. 5. Transmission electron micrographs showing iron oxide nanoparticles synthesized in planar DNA/Fe^{3+}/PVP-16 complex LB films. Image (a): $NaBH_4$ (5×10^{-4} M) was used as a reductant (incubation time 2 h). Image (b): $NaBH_4$ (5×10^{-4} M) was used as a reductant (incubation time 1 h). Image (c): ascorbic acid (10^{-3} M) was used as a reductant.

gates (Fig. 4b) when sodium borohydride and ascorbic acid were used as reductants for generation of nanoparticles. The use of DNA/Fe^{3+}/PVP-16 complex films as precursors (with other identical chemical procedures and conditions) resulted in generation of quasi-linear aggregated (Fig. 5a) and chain-like arrays of small iron oxide nanoparticles (Fig. 5b,c). Analogous effect was observed when semiconductor CdS nanoparticles were generated in cadmium stearate LB film (Fig. 6a) and in DNA/Cd^{2+}/PVP-16 complex film (Fig. 6b,c). The data obtained give evidence for the important role of DNA molecules in spatial organization of inorganic nanoparticles generated in DNA complexes what opens possibility for use of such complexes as nanoreactors for fabrication of organized planar hybrid organic-bio-inorganic nanostructures.

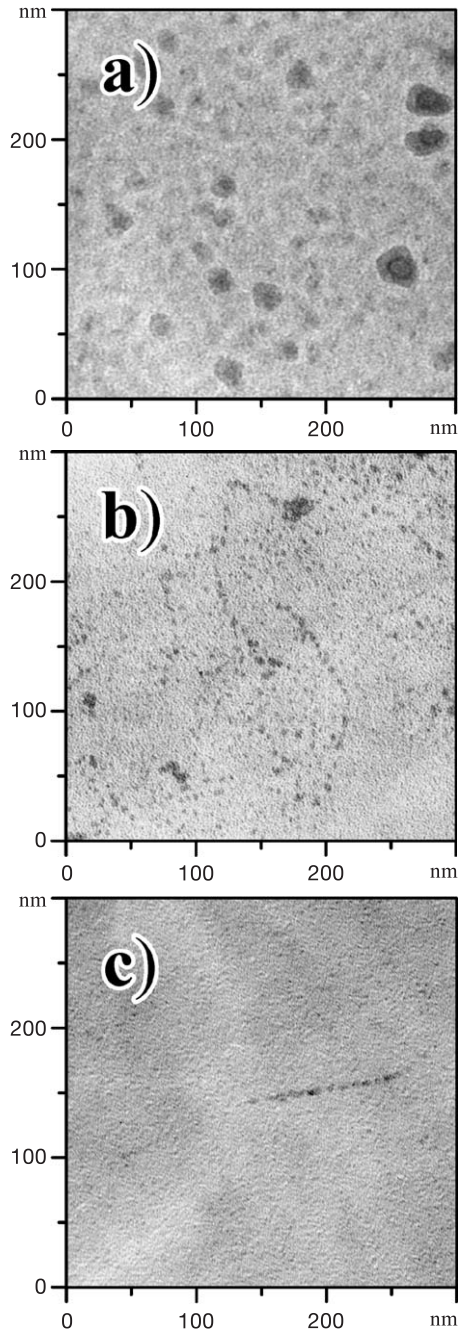

Fig. 6. Transmission electron micrographs showing CdS nanoparticles and nanostructures grown in planar supramolecular nanoreactors. Image (a): CdS nanoparticles grown in multilayer cadmium stearate LB film. Image (b): CdS nanoparticles grown in DNA/Cd^{2+}/PVP-16 complex LB film. Image (c): CdS nanowire grown in DNA/Cd^{2+}/PVP-16 complex LB film.

4. Conclusions

Effects of 2-D nanoscale supramolecular organization and patterning were observed in the amphiphilic polycation monolayer and planar DNA/amphiphilic polycation complexes formed at the air-aqueous phase interface. The effects were dependent on the amphiphilic polyelectrolyte monolayer state during the DNA binding. Planar polymeric complex films with integrated DNA and inorganic building blocks as semiconductor (CdS) and iron oxide nanoparticle quasi-linear arrays and nanowires were formed successfully. The data obtained give evidence for the effectiveness of interfacial monolayer techniques for investigation of mechanisms of structural transformations in the processes of DNA complexation with cationic compounds. Such techniques can also be perspective for creation of planar DNA-based self-organized polymeric complex nanostructures with nano-scale structural ordering which can be a promising construction material for nano-scale frameworks and scaffolds. The methods developed can be perspective for design and fabrication of new controlled-morphology highly ordered planar polymeric and composite nanostructured materials, films and coatings including ultimately thin films with thickness down to a monomolecular layer.

Acknowledgements

This work was supported by Russian Foundation for Basic Researches (Grant 02-03-33158), INTAS (Grant 99-864), ISTC (Grant 1991).

References

[1] C.M. Niemeyer, Appl. Phys., A 68 (1999) 119.
[2] C.A. Mirkin, Inorg. Chem. 39 (2000) 2258.
[3] J.L. Coffer, S.R. Bigham, R.F. Pinizzotto, H. Yang, Nanotechnology 3 (1992) 69.
[4] J.L. Cofer, J. Clust. Sci. 8 (1997) 159.
[5] E. Braun, Y. Eichen, U. Sivan, G. Ben-Yoseph, Nature 391 (1998) 75.
[6] J.J. Storhoff, C.A. Mirkin, Chem. Rev. 99 (1999) 1849.
[7] T. Torimoto, M. Yamashita, S. Kuwabata, T. Sakata, H. Mori, H. Yoneyama, J. Phys. Chem., B 103 (1999) 8799.
[8] J. Richter, R. Seidel, R. Kirsch, M. Mertig, W. Pompe, H.K. Plaascshke, Adv. Mater. 12 (2000) 507.
[9] C.M. Niemeyer, M. Adler, S. Gao, L. Chi, Angew. Chem., Int. Ed. Engl. 39 (2000) 2967.
[10] Y. Maeda, H. Tabata, T. Kawai, Appl. Phys. Lett. 79 (2001) 1181.
[11] A. Kumar, V. Ramakrishnan, R. Gonnade, K. Ganesh, M. Sastry, Nanotechnology 13 (2002) 597–600.
[12] O. Harnack, W.E. Ford, A. Yasuda, J.M. Wessels, Nano Lett. 2 (2002) 919.
[13] M. Mertig, L.C. Ciacchi, R. Seidel, W. Pompe, Nano Lett. 2 (2002) 841.
[14] P.K. Hansma, V.B. Elings, O. Marti, C.E. Bracker, Science 242 (1988) 209.
[15] R.M. Fuoss, U.P. Strauss, J. Polym. Sci. 3 (1948) 246.
[16] G.B. Khomutov, S.A. Yakovenko, E.S. Soldatov, V.V. Khanin, M.D. Nedelcheva, T.V. Yurova, Membr. Cell Biol. 10 (1997) 665.
[17] J. Zhu, A. Eisenberg, R.B. Lennox, Macromolecules 25 (1992) 6547.
[18] T.H. Eickbush, E.N. Moudrianakis, Cell 13 (1978) 295.
[19] G.S. Manning, Q. Rev. Biophys. 11 (1978) 179.
[20] D. Stigter, Biophys. J. 69 (1995) 380.
[21] M.A. Batalia, E. Protozanova, R.B. Macgregor Jr., D.A. Erie, Nano Lett. 2 (2002) 269.
[22] B.J. Rackstraw, A.L. Martin, S. Stolnik, C.J. Roberts, M.C. Garnett, M.C. Davies, S.J.B. Tendler, Langmuir 17 (2001) 3185.
[23] A.T. Woolley, R.T. Kelly, Nano Lett. 1 (2001) 345.
[24] T. Thundat, D.P. Allison, R.J. Warmack, Nucleic Acids Res. 22 (1994) 4224.